

Supporting Information

Flexible near-infrared polarized photodetector based on CuPc single
crystal grown by microspacing in-air sublimation

Mengru Li,^a Qianqian Du,^{*a} Yanxun Zhang,^a Yunlong Liu,^a Wenjun Wang,^a Fengqiu
Wang,^{*b} and Shuchao Qin,^{*a}

^aKey Laboratory of Optical Communication Science and Technology of Shandong
Province, School of Physical Science and Information Engineering, Liaocheng
University, Liaocheng 252059, China

^bSchool of Electronic Science and Engineering, Ministry of Education, Nanjing
University, Nanjing 210093, China

Corresponding Authors:

*E-mail: Shuchao Qin (lcqinshuchao@126.com); Qianqian Du (dzdq0126@163.com);

Fengqiu Wang (fwang@nju.edu.cn)

S1. AFM image of the CuPc single crystal surface

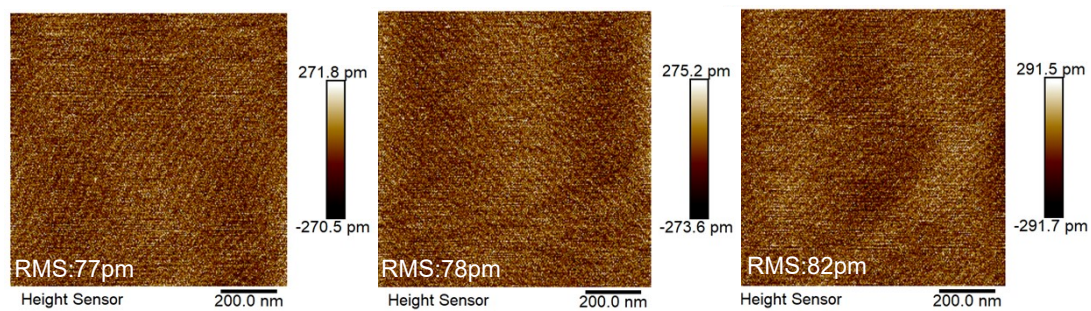


Figure S1. AFM image of the CuPc single crystal surface.

S2. Cross-polarized optical microscopy images of a CuPc single crystal

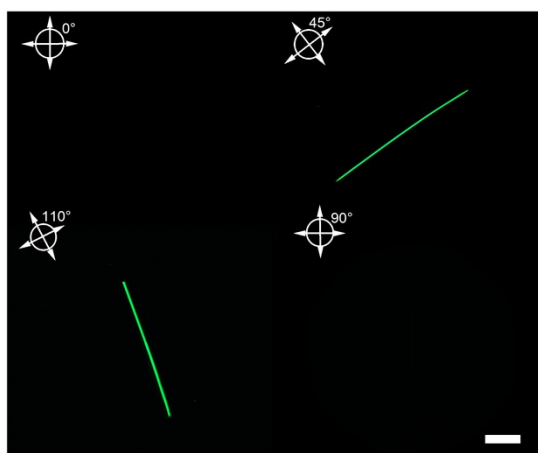


Figure S2. Cross-polarized optical microscopy images of a CuPc single crystal in different polarization directions. Scale bar: 10 μ m.

S3. SEM image of the CuPc single crystal nanowires

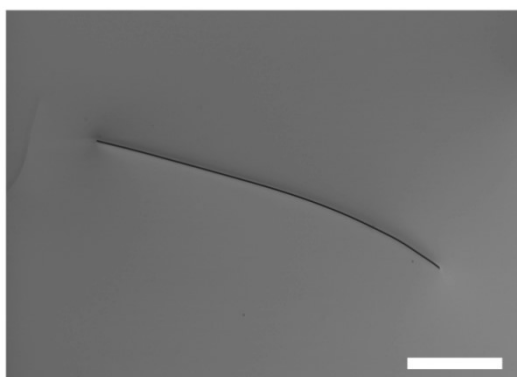


Figure S3. SEM image of the CuPc single crystal nanowires. Scale bar: 20 μm .

S4. SEM image of the CuPc device

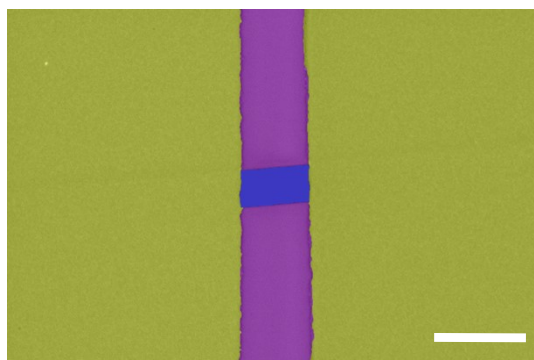


Figure S4. The false-color SEM image of CuPc transistor. Scale bar: 10 μm .

S5. CuPc single crystal FET transfer curves

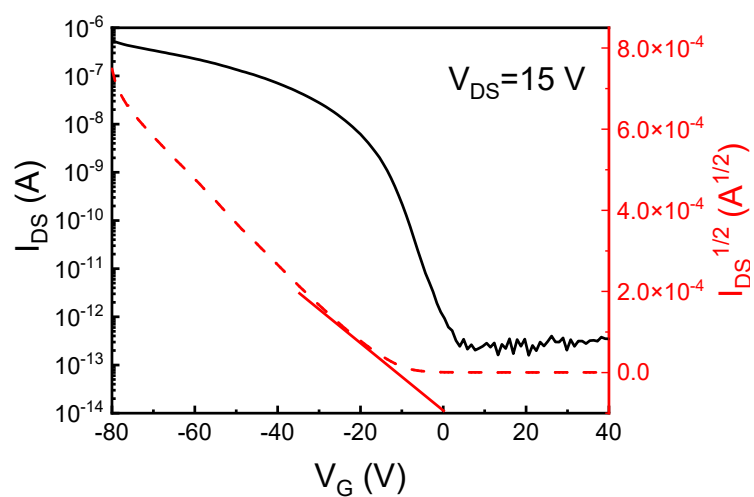


Figure S5. CuPc single crystal FET transfer curve under dark conditions.

S6. The output curve

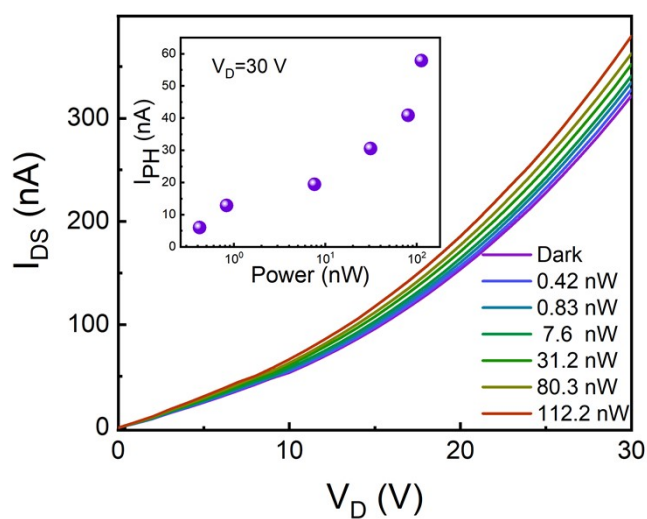


Figure S6. The output curve under different incident laser power densities (785 nm) at $V_{GS} = -60V$. Inset: Photocurrent of the device versus illumination power at $V_{DS} = 30 V$.

S7. The noise current spectral density

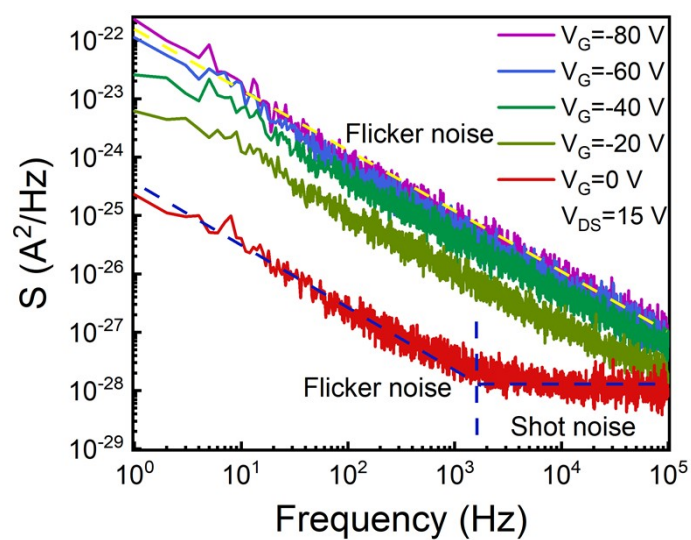


Figure S7. Noise current spectral density of the device under different gate bias.

S8. Dual gate sweeping curve

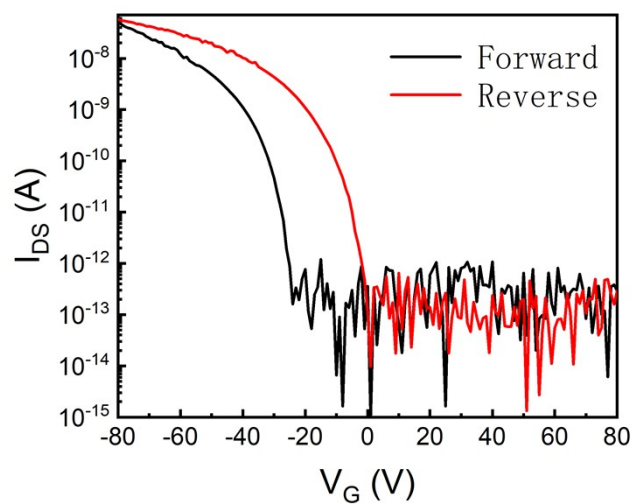


Figure S8. Transfer curve for a forward (black curve) and reverse sweep (red curve).

S9. The flattened photocurrent response of the device

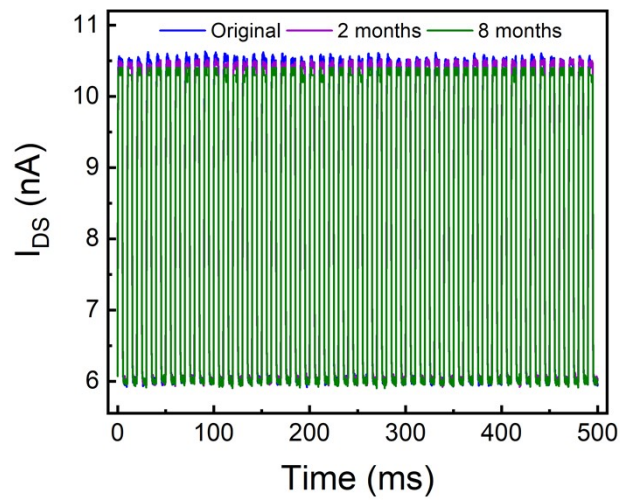


Figure S9. The flattened photocurrent response of the device as fabricated and after 0-8 months under 785nm illumination at $V_G=0V$.

S10. Schematic diagram of the single-pixel imaging measurement system

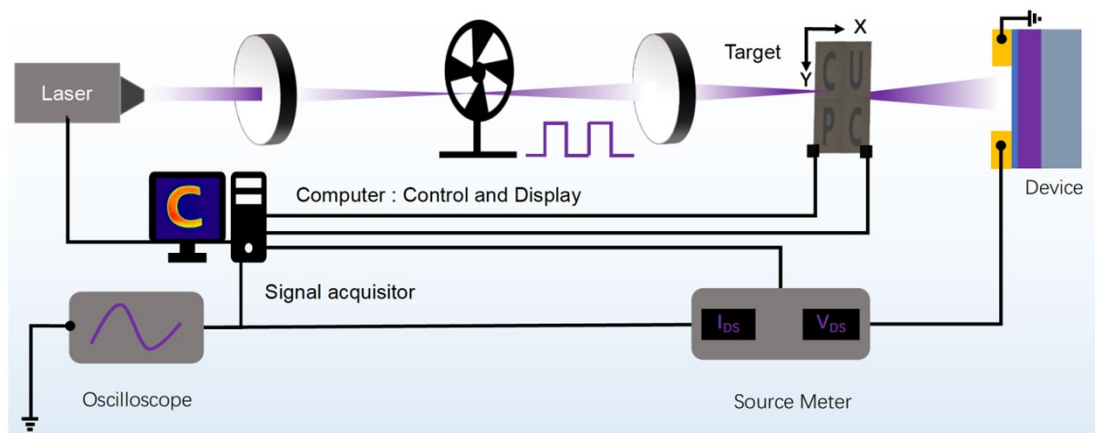


Figure S10. Schematic diagram of the single-pixel imaging measurement system. The modulated laser is focused onto the device by an objective lens. During the measurements, the measured object is moved by the step controller.